HHS Public Access

Author manuscript

Hepatology. Author manuscript; available in PMC 2021 July 28.

Published in final edited form as:

Hepatology. 2021 July ; 74(1): 411–427. doi:10.1002/hep.31698.

Efficiently restored thrombopoietin production via AMR and IL-6R induced JAK2-STAT3 signaling early after partial hepatectomy

Friedrich Reusswig[1], **Nastaran Fazel Modares**[2], **Marius Brechtenkamp**[1], **Leonard Wienands**[1], **Irena Krüger**[1], **Kristina Behnke**[2], **Melissa M. Lee-Sundlov**[3], **Diran Herebian**[4], **Jürgen Scheller**[2], **Karin M. Hoffmeister**[3], **Dieter Häussinger**[5], **Margitta Elvers**[1,*]

[1]Department of Vascular and Endovascular Surgery, Heinrich-Heine-University University Medical Center, Moorenstraße 5, 40225 Düsseldorf, Germany.

[2]Institute of Biochemistry and Molecular Biology II, Medical Faculty, Heinrich-Heine University, Düsseldorf, Germany.

[3]Blood Research Institute Versiti, Milwaukee, United States.

[4]Department of General Pediatrics, Neonatology and Pediatric Cardiology, Medical Faculty, Heinrich-Heine-University, Düsseldorf, Germany.

[5]Clinic for Gastroenterology, Hepatology and Infectious Diseases, Medical Faculty, Heinrich-Heine University, Düsseldorf, Germany.

Abstract

Thrombocytopenia has been described in most of patients with acute and chronic liver failure. Decreased platelet production and decreased half-life of platelets might be a consequence of low levels of TPO in these patients. Platelet production is tightly regulated to avoid bleeding complications after vessel injury and can be enhanced under elevated platelet destruction as observed in liver disease. Thrombopoietin (TPO) is the primary regulator of platelet biogenesis and supports proliferation and differentiation of megakaryocytes. Recent work provided evidence for the control of TPO mRNA expression in liver and bone marrow by scanning circulating platelets. The Ashwell-Morell receptor (AMR) was identified to bind desialylated platelets to regulate hepatic thrombopoietin (TPO) production via JAK2-STAT3 activation. 2/3 partial hepatectomy (PHx) was performed in mice. Platelet activation and clearance by AMR/JAK2/STAT3 signaling and TPO production was analyzed at different time points after PHx. Here, we demonstrate that PHx in mice led to thrombocytopenia and platelet activation defects leading to bleeding complications but unaltered arterial thrombosis in these mice. Platelet counts were rapidly restored via up-regulation and crosstalk of the AMR and the IL-6 receptor to induce JAK2-

[*]**Correspondence:** Margitta Elvers, Ph.D., Department of Vascular and Endovascular Surgery, Experimental Vascular Medicine, Heinrich-Heine University Medical Center, Düsseldorf, Germany. Phone: +49 (0)211 81-08851, Fax: +49 (0)211 81-17498. margitta.elvers@med.uni-duesseldorf.de.

Author contributions

JS, KMH, DH and ME conceived the project, designed the experiments, analyzed data and wrote the manuscript. FR, KV, NFM, MB, LW, MML and DH performed experiments and analyzed data. IK conducted animal experiments.

Competing interests

There are no competing interests to declare.

STAT3-TPO activation in the liver accompanied by an increased number of megakaryocytes in spleen and bone marrow before liver was completely regenerated. Conclusion: The AMR/IL-6R-STAT3-TPO signaling pathway is an acute phase response to liver injury to reconstitute hemostasis. Bleeding complications were due to thrombocytopenia and platelet defects induced by elevated PGI_2, NO and bile acid plasma levels early after PHx that might be also causative for the high mortality in patients with liver disease.

Keywords

Platelets; hepatocytes; IL-6; liver regeneration; bleeding

Introduction

An adequate supply of fully functional platelets is necessary to achieve hemostasis after vascular damage. Platelet production is tightly regulated to avoid either bleeding or arterial thrombosis according to low or high platelet counts. In humans ~10^{11} platelets are daily produced and removed. However, platelet production can be enhanced under conditions of platelet destruction, e.g. in response to acute infection. The primary regulator of platelet production is thrombopoietin (TPO) that supports the survival, proliferation and differentiation of megakaryocytes, the platelet precursors [1]. In general, the plasma concentration of TPO is inversely related to the mass of platelets and megakaryocytes. However, the mechanisms how circulating TPO levels are controlled have been discussed for decades. While some researchers believe that TPO levels in plasma are maintained by its uptake and metabolism by Mpl receptors on platelets and megakaryocytes [2, 3], others provided evidence for sensing circulating platelet levels to control TPO mRNA expression in liver and bone marrow (BM) [4, 5]. Recently, Grozovsky and colleagues have highlighted the role of sialic acid loss and platelet removal by the hepatic Ashwell Morell receptor (AMR). They found platelet production to be regulated by the AMR that controls hepatic TPO production via the JAK2/STAT3 signaling pathway[6]. Loss of sialic acid determines the life span of platelets that triggers platelet removal by hepatic AMR. Desialylated platelets bind to the AMR to induce hepatic expression of TPO mRNA and protein to regulate platelet production.

Thrombocytopenia has been described in most of patients with acute and chronic liver failure that are causative for bleeding problems in these patients [7]. Decreased platelet production and decreased half-life of platelets might be a consequence of low levels of TPO in these patients [8–11]. Besides, platelet activation defects have been reported in experimental mice [12] and patients with cirrhosis [13–16]. In bile duct ligated (BDL) mice, elevated nitric oxide and prostacyclin levels induced phosphorylation of the platelet inhibitor vasodilator-stimulated phosphoprotein (VASP) leading to prolonged platelet activation defects and defective hemostasis in BDL mice [17, 18].

However, platelet production following activation of the AMR and JAK2/STAT3 signaling was reported in healthy individuals. The consequences of cytokine signaling and reduced platelet life span upon liver injury are not known to date. Moreover, regulation of plasma

TPO levels by hepatic AMR has not been investigated in mice with reduced liver tissue e.g. after partial hepatectomy (PHx).

In this study, we provide first evidence that enhanced platelet turnover and cytokine signaling synergistically control TPO homeostasis in the remaining liver tissue via activation of the AMR and IL-6R to restore platelet counts in the early phase after PHx in mice. Platelet activation defects were moderate and occurred early after PHx resulting in bleeding complications at day 1 and day 3 after PHx, while arterial thrombosis was not prevented.

Material and Methods

Animals.

Specific pathogen-free C57BL/6J mice were obtained from Janvier Labs. *IL-6r*$^{-/-}$ and *Asgr2*$^{-/-}$ mice were obtained from Jackson Laboratory and the Animal Facility of the Heinrich-Heine University of Düsseldorf. Experiments were performed with male mice in the age of 8–16 weeks. All animal experiments were conducted according to the Declaration of Helsinki and the guidelines from Directive 2010/63/EU of the European Parliament on the protection of animals. The protocol was approved by the Heinrich-Heine-University Animal Care Committee and by the State Agency for Nature, Environment and Consumer Protection of North Rhine-Westphalia (LANUV, NRW; Permit Number 84–02.04.2015.A462, O 86/12 and 84–02.04.2016.A493).

Results

PHx in mice is associated with thrombocytopenia and anemia at early time points.

PHx was performed and 2/3 of the liver in wildtype (WT) mice was removed. Sham operated control mice underwent the same surgical procedure without ligation and removal of liver tissue. Blood cell counts and liver weight were analyzed in both groups. Platelet counts were significantly reduced by 16.411% 1 day after surgery and fully restored 7 days after PHx (Fig. 1A) while platelet size was enhanced at 1 and 3 days after surgery (Fig. 1D) as compared to platelets from sham controls. Likewise, red blood cell (RBC) count was significantly reduced by 8.75% 1 day after PHx and restored 7 days after PHx (Fig. 1B) while no major alterations in white blood cell counts were detected (Fig. 1C). Liver weight ratio to body weight was significantly reduced 1, 3 and 7 days after PHx. In line with recent data, liver was fully regenerated 14 days post PHx (Fig. 1E) [19].

PHx provokes platelet activation defects and reduced thrombus formation resulting in impaired hemostasis at early phase after PHx.

A detailed analysis of platelets 1 day post PHx revealed unaltered glycoprotein exposure at the surface of platelets isolated from PHx mice (Fig. 1F). Platelet activation was analyzed by antibody binding to activated integrin αIIbβ3 (fibrinogen receptor) and determination of P-selectin exposure as marker for degranulation using flow cytometry (Fig. 1G–I). Reduced integrin activation restricted to stimulation of platelets with collagen-related peptide (CRP) that activates the major collagen receptor glycoprotein (GP) VI was detected (Fig. 1G) while the number of integrin αIIbβ3 at the platelet surface was reduced in response to CRP and

thrombin (Fig. 1H). Degranulation of platelets in hepatectomized mice was significantly reduced in response to the second wave mediators ADP+U46619 (thromboxane analog), intermediate and high concentrations of CRP, low and intermediate concentrations of the thrombin receptor activator PAR4 peptide and low dose of thrombin (Fig. 1I). To analyze platelet activation under more physiological condition, flow chamber experiments were performed. Platelet adhesion and three-dimensional thrombus formation was analyzed at arterial shear rates (1.000 sec^{-1}, 1.700 sec^{-1}) using collagen coated coverslips (Fig. 1J). Thrombus formation was significantly reduced when we perfused whole blood isolated from hepatectomized mice through the chamber compared to whole blood from sham controls.

Next, we investigated if platelet activation defects are relevant *in vivo*. To this end, bleeding time experiments were conducted and time was recorded when bleeding stops after cutting the tail tip of mice. As shown in Fig. 1K, bleeding time was significantly prolonged 1 day after PHx compared to sham controls (Fig. 1K). In addition, we examined arterial thrombus formation in mice 1 day after PHx. Fe_3Cl-induced injury of the carotid artery led to occlusion of the vessel after 439 sec ± 57 in hepatectomized mice and 409 sec ± 29 in sham controls (Fig. 1K) suggesting no major alterations in arterial thrombosis after PHx in mice despite defective hemostasis.

Further analysis of platelet activation and thrombus formation 3 days after PHx revealed significantly enhanced the exposure of GPIbα and integrin β3 at the platelet surface of hepatectomized mice in contrast to 1 day after PHx (Fig. 2A), whereas integrin αIIbβ3 activation was still significantly reduced in response to intermediate and high concentrations of CRP but unaltered in response to G-protein coupled receptor activation such as thrombin and ADP/U46619 (Fig. 2B). In contrast to day 1 post PHx, the exposure of integrin β3 was significantly enhanced in resting and ADP stimulated platelets from PHx mice compared to sham controls (Fig. 2C). P-selectin exposure as marker for degranulation was only moderately but still significantly reduced at the surface of platelets from PHx mice when they were stimulated with CRP or thrombin (Fig. 2D). Moderate platelet activation defects translated into impaired thrombus formation under flow *ex vivo* using a shear rate of 1.000 sec^{-1} but not at a shear rate of 1.700 sec^{-1} (Fig. 2E). Moreover, bleeding time was still significantly reduced but to a lesser extent compared to 1 day after PHx (Fig. 2F). However, no differences in platelet activation and thrombus formation were detected 7 (Supporting Fig. 1, A–E) and 14 days (Supporting Fig. 2, A–E) after PHx.

Defective platelet activation after PHx is caused by elevated nitric oxide, prostacyclin and bile acid plasma levels.

To investigate the mechanisms responsible for reduced platelet activation and thrombus formation 1 and 3 days after PHx, we analyzed the phosphorylation of VASP, a negative regulator of platelet activation. VASP can be phosphorylated at Ser157 via protein kinase (PK)A that is activated by prostaglandin I2 (prostacyclin, PGI_2) and at Ser239 via PKG which is activated by nitric oxide (NO) [18, 20, 21]. We started to measure the plasma concentration of PGI_2 by ELISA. At day 1 post PHx, PGI_2 plasma levels were significantly enhanced and returned to normal levels at day 3 post PHx compared to sham controls (Fig. 3A). Further, we investigated the stable NO metabolites nitrate and nitrite by ELISA. At 1

day after surgery levels of NO metabolites were enhanced while no major alterations were observed 3 days post PHx (Fig. 3B). According to enhanced PGI_2 plasma levels, we detected enhanced phosphorylation of VASP at Ser157 in platelets of hepatectomized mice compared to controls using Western blot analysis. However, no major alterations in the phosphorylation of VASP at Ser157 were detected 3 days post PHx (Fig. 3, C and D, Supporting Fig. 3, A and B). In line with enhanced NO metabolites enhanced VASP phosphorylation at Ser239 was detected in platelets from hepatectomized mice stimulated with the corresponding NO analogue sodium nitroprusside (SNP). However, no alterations were detected 3 days post PHx (Fig. 3, E and F, Supporting Fig. 3, A and B).

Previously we have shown that enhanced plasma levels of bile acids account for platelet activation defects in bile duct ligated mice (17). Therefore, we analyzed total plasma levels of bile acids in hepatectomized mice. Enhanced total bile acid plasma levels were detected in mice at day 1 and 3 after PHx compared to sham controls consistent with published data (Fig. 3G) [22]. To provide evidence that bile acids induce platelet activation defects, we incubated whole blood with different tauro-conjugated endogenous bile acids since especially taurine-conjugated bile acids are present in the plasma of hepatectomized mice (Supporting Fig. 4A) and analyzed platelet adhesion and thrombus formation at arterial shear rates *ex vivo*. Incubation of whole blood with the hydrophilic bile acids taurocholate (TC) or taurochenodeoxycholate (TCDC) did not alter thrombus formation under flow while the addition of hydrophobic taurodeoxycholate (TDC) or taurolithocholate (TLC) to whole blood led to significantly reduced thrombus formation under flow compared to controls (Fig. 3H). However, no alterations were detected when platelets were incubated with 50 μM TC, TCDC, TDC and TLC, respectively and platelet aggregation in response to PAR4 peptide and CRP was analyzed under static conditions (Supporting Fig. 4, B–E). These results suggest that hydrophobic bile acids affect platelet activation under dynamic conditions beside high plasma concentrations of PGI_2 and NO.

Efficiently restored thrombopoietin production is mediated via desialylated platelet uptake into the diseased liver by the AMR and JAK2 and STAT3 signaling.

TPO the major regulator of platelet production is primarily produced in the liver [23]. The paradox early restoration of platelet counts 3 days after PHx, a time point where the liver tissue is still strongly reduced in hepatectomized mice, prompted us to analyze TPO production in the remaining liver tissue in further detail. Senescent desialylated platelets stimulate TPO production [6]. Therefore, we first characterized circulating platelets for phosphatidylserine exposure (PS) at the platelet surface as marker for pro-coagulant activity which might be also important for recognition and subsequent removal of senescent platelets [24]. At early time points after surgery with enhanced levels of PGI_2, NO and bile acids, no major alterations in PS were detected between platelets from hepatectomized mice and sham controls (Fig. 4A). However, 7 days after PHx, decreased PS exposure on the surface of PHx platelets was detected following platelet activation with CRP. Reduced PS returned to basal levels 14 days after surgery when liver tissue regeneration was completed. Aging platelets lose sialic acid, the terminal carbohydrate moiety that covers the underlying galactose residues, a ligand for the hepatic AMR. Desialylated aged platelets are removed from the circulation by hepatic AMR to regulate TPO production via JAK2-STAT3 [25]. We

speculated that platelets following PHx may be cleared in the liver via glycan dependent mechanisms. Thus, we next investigated the sialic acid content of circulating platelets post PHx. The fraction of desialylated platelets was examined by platelet lectin binding such as *Ricinus communis* agglutinin (RCA-1), a lectin that recognizes terminal galactose residues (Fig. 4B). Reduced lectin binding was detected 1 day post PHx reflecting a reduced percentage of desialylated platelets. This suggests that desialylated platelet clearance is accelerated at early time points after PHx (Fig. 4B). In contrast, we detected enhanced lectin binding of platelets from hepatectomized mice at day 7 after surgery. Thiazole orange staining revealed an elevated number of newly produced platelets 7 days after PHx but no alterations at any other time point (1d, 3d, 14d, Fig. 4C). These results suggest a reciprocal relationship between two clearance mechanisms at early and late time points after PHx: 1st, reduced desialylated platelet clearance at early time points (day 1) and 2nd, increased clearance of PS-positive platelets at late time points (day 7), a notion that is supported by galactose exposure at day 1 and reduced PS exposure with increased RCA-1 binding of PHx platelets at day 7. Enhanced numbers of RNA-rich, newly produced platelets 7 days after PHx (Fig. 4, A–C), further supports the notion. Platelet clearance can be also induced by vWF binding to GPIb leading to the release of neuraminidase and subsequent platelet desialylation [26]. Analysis of neuraminidase (Neu)-1 expression after PHx revealed that platelets of PHx mice have a higher Neu-1 expression on their surface compared to sham controls (Supporting Fig. 5A). *In vitro,* vWF binding to GPIb induce by the snake venom botrocetin led to increased Neu-1 expression in sham operated mice while the upregulation of Neu-1 was almost inhibited in PHx mice (Fig 4D). At the same time, no difference in the plasma activity of Neu-1 was detected (Supporting Fig. 5B). This effect of vWF-GPIb mediated increase of Neu-1 expression was confirmed by blocking vWF-binding to GPIb (Fig 4D). In addition, Neu-1 expression was also reduced when platelets from PHx mice were stimulated with 1 μg CRP. However, Neu-1 activity was unaltered while vWF plasma levels were enhanced in mice 24h after PHx compared to sham controls (Supporting Fig. 5A–C). Thus, reduced platelet activation early after PHx probably leads to reduced neuraminidase exposure that might account for the reduced number of desialylated platelets in the circulation of PHx mice suggesting that shear stress induced vWF binding at least partially contributes to the reduced number of lectin positive platelets that were detected after PHx.

Concomitant with reduced lectin binding of circulating platelets we identified platelets invading into the liver at day 1 and to a lesser extent at day 3 (Fig. 4E). This might be due to the binding of desialylated platelets to the AMR inducing hepatic TPO gene transcription and translation to regulate platelet production [6] in the remaining liver tissue early after PHx. Therefore, gene expression of both subunits of the AMR, *Asgr1* and *Asgr2,* were examined in the remaining liver tissue at different time points after surgery. Expression of the *Asgr1* was enhanced with a peak at 6 hours and a smaller peak at 3 days while *Asgr2* expression was enhanced only at 3 days after PHx (Fig. 4, F and G). Different reports demonstrated that IL-6 could stimulate thrombopoiesis through TPO in an inflammatory environment [27, 28]. Here, the expression of the IL-6 receptor (IL-6R) in the remaining liver tissue was measured. In line with increased *Asgr1/2* expression in the remaining liver, expression of *Il-6r was* elevated in the liver of hepatectomized mice with a similar

expression pattern observed in *Asgr1* expression (Fig. 4H). Enhanced expression of *Asgr1/2* and *Il-6r* was accompanied by enhanced *Tpo* expression 6 hours and 3 days post PHx (Fig. 4I) despite a significant reduction in liver weight to body weight observed at 1 day to 3 days after PHx (Fig. 1E). In plasma, enhanced TPO levels were detected at day 1 post PHx compared to sham controls (Fig. 4J). A significant elevation of synthesized and released TPO was also evident at day 3 when relative TPO levels were measured in comparison to total liver mass (Fig. 4K). AMR signals through Janus kinase 2 (JAK2) and the acute phase response signal transducer and activator of transcription 3 (STAT3)[6]. Thus, the phosphorylation of JAK2 and STAT3 at different time points after PHx was examined (Fig. 4L). In line with enhanced plasma TPO levels, phosphorylation of JAK2 and STAT3 was enhanced 1 day post PHx using Western blot (Fig. 4, L–N, Supporting Fig. 6, A and B). Hence, the data show that glycan-dependent clearance of platelets is occurring in the liver followed by upregulation of AMR-dependent JAK2-STAT3 regulated TPO production.

Enhanced AMR-JAK2-TPO signaling after PHx provokes elevated megakaryopoiesis in spleen and bone marrow.

Megakaryopoiesis is mainly controlled by TPO. To investigate if increased AMR-JAK2-TPO signaling affects megakaryopoiesis in spleen and bone marrow to restore platelet counts, spleen weight to body weight ratio was measured at different time points after PHx. The ration was significantly increased 3 and 7 days after PHx compared to sham controls (Fig. 5, A and B). Accordingly, the number of megakaryocytes in spleen and bone marrow was enhanced 3 and 7 days after PHx (Fig. 5, E–H). In line with splenomegaly, clearance of platelets was observed by an increased fraction of platelets in the spleen of mice 7 days post PHx compared to sham controls suggesting clearance of PS-positive platelets at this time point by splenic macrophage scavenger receptors (Fig. 5, C and D). This accelerated platelet sequestration into spleen may explain the increase in spleen size at later time points. Taken together, the increase in megakaryocytes in spleen and bone marrow supports the increased number of produced platelets. The data further suggest that enhanced clearance of PS-positive platelets in the spleen either allows platelets to circulate with enhanced RCA binding to platelets at day 7 post PHx or young platelet express more terminal galactose that is not recognized by galactose receptors such as the AMR (Fig. 4, B and C).

Cytokine signaling via the IL-6R and STAT signaling plays a crucial role in TPO homeostasis after PHx.

IL-6R expression is significantly increased 6 hours after PHx (Fig. 4G). To investigate in further detail, how IL-6R signaling is involved in TPO homeostasis and restoration of platelet counts after PHx, we analyzed *IL-6r*$^{-/-}$ mice at steady state (native) and after PHx (up to 24 hours after surgery because of high mortality of *IL-6r*$^{-/-}$ mice). *IL-6r*$^{-/-}$ *mice* showed significantly enhanced platelet counts under native conditions compared to wildtype (WT) mice. However, platelet counts were strongly reduced in *IL-6r*$^{-/-}$ mice as well as in WT mice 1 day after PHx (Fig. 6A). Platelets from IL-6R deficient mice showed enhanced size under native conditions and after PHx compared to WT controls as measured by flow cytometry (Fig. 6B). Thiazole orange staining revealed an elevated number of young platelets in IL-6R deficient mice after PHx compared to native conditions as well as to WT mice after PHx (Fig. 6C). A significantly reduced number of desialylated platelets in IL-6R

deficient mice under native conditions provided evidence for an enhanced platelet clearance of desialylated platelets (Fig. 6D). The expression of the AMR subunits *Asgr1* and *Asgr2* was significantly up-regulated in IL-6R deficient mice under native conditions. Early after PHx, the expression of the subunit *Asgr1* was enhanced as well supporting the notion of increased desialylated platelet uptake by the AMR (Fig. 6E). No difference was detected in the expression of the *Asgr2* at any time point after PHx (Fig. 6F). Interestingly, *Il-6r* was likewise up-regulated in the liver of native $Asgr2^{-/-}$ mice (Supporting Fig. 7F). Accordingly, *Tpo* expression in the liver of native mice and in the remaining tissue after PHx was significantly enhanced in IL-6R deficient mice (Fig. 6G). We next analyzed the downstream signaling pathway following AMR activation in the liver. Phosphorylation of JAK2 and STAT5 was indistinguishable between WT and IL-6R deficient mice under native conditions while the phosphorylation of STAT-3 was significantly reduced in IL-6R deficient mice (Fig. 6, H–L, Supporting Fig. 7A). However, 1 day post PHx, phosphorylation of STAT3 was up-regulated in both groups while STAT5 seemed to be not regulated after PHx. However, the phosphorylation of JAK2 was significantly enhanced in the liver of WT but only by trend in IL-6R deficient mice (Fig. 6, H and I, Supporting Fig. 7B). In line with enhanced *Tpo* expression in the liver of IL-6R knock-out mice, enhanced TPO protein levels were observed in the livers of WT and IL-6R deficient mice isolated 1 day after PHx in (Fig. 6J, Supporting Fig. 7B). Accordingly, TPO plasma levels were enhanced in IL-6R knock-out mice under native conditions and 1 day after PHx. However, plasma levels of TPO were significantly lower 12 hours after PHx compared to WT controls suggesting attenuated release of TPO from the liver into the circulation (Fig. 6K).

Subsequently, we analyzed if accelerated desialylated platelet clearance affects the number of megakaryocytes in the bone marrow and spleen of IL-6R deficient mice 1 day post PHx as suggested by decreased number of RCA-1 binding platelets at early time points post PHx (Fig. 4C). An increased number of megakaryocytes was observed in the bone marrow and in spleen of IL-6R deficient mice under native conditions compared to WT controls (Fig. 6, L and M). After PHx, the number of megakaryocytes was significantly enhanced in spleen but not in bone marrow of IL-6R deficient mice (Fig. 6, L and M). In line with unaltered counts of megakaryocytes in bone marrow and spleen between sham controls and PHx mice 1 day after PHx (Fig. 5, C–F), no differences were observed in native WT mice compared to 1 day after PHx. Increase in bone marrow megakaryocytes in response to TPO stimulation was only overserved at 3–7 days post PHx. Spleen weight was comparable between WT and IL-6R knock-out mice under native conditions and after PHx (Supporting Fig. 7E). However, platelet sequestration into the spleen of $IL\text{-}6r^{-/-}$ mice was enhanced under native conditions and 1 day post PHx compared to WT controls. (Supporting Fig. 7, C and D). The unaltered spleen weight in IL-6R deficient mice points to enhanced platelet destruction in IL-6R deficient mice as suggested by a significantly reduced number of desialylated platelets in IL-6R deficient mice under native conditions (Fig. 6D).

To analyze if recombinant IL-6 is able to stimulate thrombopoiesis after PHx, we treated mice with recombinant hyper-IL6 (hIL-6) because hIL6 has a 10 times higher bioactivity than IL-6 alone and a longer bioavailability *in vivo* [29]. While no differences in platelet counts could be observed after hIL6 treatment, enhanced platelet size was measured in hIL-6 treated mice compared to controls (Supporting Fig. 8A–B). Additionally, hIL-6 application

induced enhanced TPO plasma levels, which was accompanied by an enhanced number of MKs in the spleen but not in the bone marrow of hIL-6 treated mice 24h after operation (Supporting Fig. 8C–G). These results give a first indication that treatment with recombinant IL-6 induces thrombopoiesis after PHx. However, further experiments in near future are needed to clarify the role of IL-6 signaling for thrombopoiesis.

Discussion

Here we report that platelet counts were rapidly restored after PHx via the AMR/IL-6R-JAK2-STAT signaling pathway leading to elevated TPO expression and release from the remaining liver tissue to reconstitute hemostasis at early time points when liver tissue has not been fully regenerated. This strongly suggests that enhanced platelet turnover and cytokine signaling synergistically control TPO homeostasis in the remaining liver tissue. In addition, we provide evidence that platelet activation defects were moderate due to elevated plasma levels of NO, PGI_2 and bile acids early after PHx leading to defective hemostasis at day 1 and day 3 after surgery.

This is the first report to show how TPO homeostasis and restoration of platelet counts is regulated in mice with significantly reduced liver tissue. Thrombocytopenia in liver disease develops as a consequence of decreased platelet production, increased destruction/platelet turnover and increased consumption or splenic sequestration [7, 30], all markers that were also found in mice after PHx. Depressed TPO levels in chronic liver diseases result in a reduced rate of platelet production as TPO regulates both platelet production and maturation which is impaired in chronic liver disease [30]. Thus, regulation of TPO is a long-known factor in liver disease. As the liver is the major site of TPO production [31] it is reasonable to expect decreased plasma levels in patients with liver disease. Indeed, TPO mRNA levels in the liver were slightly decreased in cirrhosis [32] and/or chronic hepatitis [33–35], and normalize after liver transplantation [36, 37]. However, increased serum TPO levels in hepatitis C and cirrhotic patients also have been published [11, 38]. This might be due to the time point of the TPO measurements since we observed a bi-phasic upregulation of TPO expression at early time points after PHx with increased cytokine signaling that might be different e.g. in chronic liver failure with chronic inflammation.

In liver disease, thrombocytopenia is an indicator of advanced disease and poor prognosis. However, thrombocytopenia is often accompanied by platelet activation defects, and this all together might contribute to the bleeding diathesis in liver failure [30, 39]. Enhanced bleeding risk is described in patients with liver transplantation [39]. However, high platelet counts are beneficial for the outcome after liver resection and liver transplantation not only with regard to bleeding complications but also due to their ability to promote liver regeneration [40]. Here we report that bleeding complications in mice are related to decreased platelet counts and platelet activation defects at day 1 and 3 after PHx but probably also due to a reduction of coagulation factors which are produced in the liver. However, the remaining liver tissue can rescue platelet counts by up-regulation of the AMR/IL-6R-JAK2-STAT signaling pathway already 6h after surgical treatment, at least in mice (Fig. 4, E–H). Since PGI_2, NO and bile acid levels normalize already at 3 days (NO, PGI_2, Fig. 3, A and B) and 7 days (bile acids, Fig. 3G) after PHx, platelet counts and platelet

activation is already rehabilitated 7 days after PHx when liver regeneration is not fully completed (Fig. 1E). This might be different in chronic liver disease in patients or experimental mice, e.g. in BDL mice where bile acids circulate in plasma for weeks and platelet activation defects including defective hemostasis were detected until 21 days after bile duct ligation [17]. Interestingly, arterial thrombosis was not prevented by concomitant low platelet counts and platelet defects 1 day post PHx (Fig. 1K). However, thrombosis has been also described in patients with liver failure despite reduced synthesis of procoagulant proteins, platelet defects and bleeding complications [39, 41]. There are reports about platelet defects in knock-out mice which do protect these mice against thrombosis but do not alter hemostasis, e.g. in PLD1 deficient mice [42] suggesting that there might be co-existing processes of hemostasis that may not cause thrombosis and vessel occlusion and the other way around. To date, the recognition of circulating desialylated platelets by hepatic AMR and the regulation of TPO mRNA expression and secretion via JAK2-STAT3 signaling was shown under steady state conditions [6]. Recently, Kupffer cells were identified as the main trigger of platelet clearance. The authors described a new mechanism that includes the collaboration of the macrophage galactose lectin (MGL) with the AMR on Kupffer cells to remove desialylated platelets from the circulation in native mice [43]. To our knowledge, nothing is hitherto known about regulatory feedback mechanisms in liver disease with enhanced cytokine signaling. Thus, the underlying mechanisms are crucial for the understanding of enhanced platelet turnover/destruction and reduced platelet counts in disease. However, our data does not clearly show if hepatocytes and/or Kupffer cells are responsible for platelet clearance and TPO production after PHx. Thus, further experiments are needed in near future to identify the cell population in liver that can efficiently restore platelet counts after PHx.

Enhanced destruction of platelets has been described in liver disease and therefore is a common feature in chronic and acute liver failure [30, 39]. To date, it is completely unknown how the AMR-JAK2-STAT3 signaling pathway is regulated in liver disease. Our study shows for the first time that IL-6R signaling in the liver is involved in TPO hemostasis and megakaryopoiesis upon elevated cytokine signaling as it occurs after PHx. Thus, elevated cytokine plasma levels account for the regulation of platelet counts upon accelerated platelet clearance. Different reports suggested that IL-6 is able to stimulate thrombopoiesis through TPO in an inflammatory environment [27, 28]. This together with the fact that the AMR signaling pathway shares similarities with that of the IL-6R prompted us to investigate the role of IL-6R in TPO homeostasis in more detail. First, we detected elevated IL-6R mRNA in the liver after PHx as already observed for the AMR (Fig. 4G). IL-6R knock-out mice exhibited reduced platelet counts after PHx like WT mice but their platelets were increased in size and they had significantly more young platelets in the circulation suggesting an enhanced platelet turnover compared to WT mice. The loss of the IL-6R in liver tissue was compensated by an increase of the AMR subunits *Asgr1* and *Asgr2* mRNA, the latter only under native conditions (Fig. 6, E and F). This compensation led to excessive TPO mRNA levels in liver and plasma under native conditions and at different time points after PHx (Fig. 6G). However, the increase in TPO was not able to restore platelet counts 1 day after PHx compared to WT controls (Fig. 6A). This might be due to the dysregulation of platelet counts and enhanced platelet turnover under native conditions

reflected by an enhanced number of megakaryocytes in bone marrow and spleen (Fig. 6, L and M), enhanced platelet size and reduced desialylation of platelets leading to enhanced expression of AMR and TPO (Fig. 6, B–D). Taken together, this is the first evidence for an involvement of IL-6R signaling in TPO homeostasis and platelet count regulation in mice with reduced liver tissue under inflammatory conditions. The fact that loss of IL-6R is compensated by enhanced expression of *Asgr1/2* provides the first evidence for a cross talk between the AMR and the IL-6R to regulate TPO levels and megakaryopoiesis in bone marrow and spleen. This conclusion is strengthened by enhanced IL-6R mRNA levels in the liver of ASGR2 knock-out mice (Supporting Fig. 5D). IL-6 is critically involved in hepatocyte proliferation and liver regeneration after PHx [44, 45]. To investigate if IL-6 is able to stimulate thrombopoiesis, we treated mice with recombinant hIL-6. Elevated TPO plasma levels and an enhanced number of MKs in the spleen of hIL-6 treated mice 24h after PHx gave a first indication that treatment with recombinant IL-6 induces thrombopoiesis after PHx. As recent studies revealed that IL-6 trans-signaling through the soluble IL-6/IL-6R complex controls liver regeneration besides the classical IL-6 signaling [46], we used the recombinant fusion protein hIL-6 that consists of the sIL-6R and IL-6 that mimics IL-6 trans-signaling [47]. In the study of Behnke *et al* it was already shown that administration of hIL 6 results in improved liver regeneration by Ki67 and phospho-H3 staining in liver tissue after PHx [48]. Taken together, it will be of great interest to investigate the effects of recombinant IL-6 on the restoration of platelet counts and megakaryopoiesis in further detail. Therefore, the analysis of different models of IL-6 signaling such as IL-6R knock-out, recombinant hyperIL-6 or GP130 transgenic mice could be helpful to shed light on the impact of IL-6 (trans-) signaling on thrombopoiesis after PHx or other inflammatory diseases that are accompanied by thrombocytopenia. Of note, we here used IL-6R deficient mice until 24 hours after PHx as of the high mortality rate in these mice due to the important role of the IL-6 signaling pathway after PHx.

In conclusion, our study identifies the AMR/IL-6R-STAT3-TPO signaling pathway as a highly efficient and acute phase response to liver injury, cytokine signaling and loss of liver tissue to restore platelet count and function. Thrombocytopenia and platelet activation defects induced by enhanced PGI_2, NO and bile acid plasma levels are responsible for bleeding complications early after PHx that might also be causative for bleeding problems and high mortality in patients with liver disease.

Supplementary Material

Refer to Web version on PubMed Central for supplementary material.

Acknowledgements

We thank Martina Spelleken, Vanessa Herbetz and Nicole Eichhorst for excellent technical assistance.

Financial Support:

This study was supported by grant from the Deutsche Forschungsgemeinschaft, Sonderforschungsbereich 974, Düsseldorf.

Abbreviations

TPO	thrombopoietin
AMR	ashwell-morell receptor
IL-6R	interleukin-6 receptor
PHx	partial hepatectomy
JAK2	januskinase 2
STAT3	signal transducer and activator 3
STAT5	signal transducer and activator 5
VASP	vasodilator-stimulated phosphoprotein
PGI_2	prostaglandin I_2, prostacyclin
NO	nitric oxide
CRP	collagen-related peptide
U46619	thromboxane A2 analogue

References

1. Kaushansky K, The molecular mechanisms that control thrombopoiesis. J Clin Invest, 2005. 115(12): p. 3339–47. [PubMed: 16322778]
2. Fielder PJ, et al., Regulation of thrombopoietin levels by c-mpl-mediated binding to platelets. Blood, 1996. 87(6): p. 2154–61. [PubMed: 8630374]
3. Kuter DJ and Rosenberg RD, The reciprocal relationship of thrombopoietin (c-Mpl ligand) to changes in the platelet mass during busulfan-induced thrombocytopenia in the rabbit. Blood, 1995. 85(10): p. 2720–30. [PubMed: 7742532]
4. McCarty JM, et al., Murine thrombopoietin mRNA levels are modulated by platelet count. Blood, 1995. 86(10): p. 3668–75. [PubMed: 7579332]
5. McIntosh B and Kaushansky K, Transcriptional regulation of bone marrow thrombopoietin by platelet proteins. Exp Hematol, 2008. 36(7): p. 799–806. [PubMed: 18410987]
6. Grozovsky R, et al., The Ashwell-Morell receptor regulates hepatic thrombopoietin production via JAK2-STAT3 signaling. 2015. 21(1): p. 47–54.
7. Lisman T and Luyendyk JP, Platelets as Modulators of Liver Diseases. Semin Thromb Hemost, 2018. 44(2): p. 114–125. [PubMed: 28898899]
8. Aoki Y, Hirai K, and Tanikawa K, Mechanism of thrombocytopenia in liver cirrhosis: kinetics of indium-111 tropolone labelled platelets. Eur J Nucl Med, 1993. 20(2): p. 123–9. [PubMed: 8440268]
9. Schmidt KG, et al., Kinetics and in vivo distribution of 111-In-labelled autologous platelets in chronic hepatic disease: mechanisms of thrombocytopenia. Scand J Haematol, 1985. 34(1): p. 39–46. [PubMed: 3918341]
10. Stein SF and Harker LA, Kinetic and functional studies of platelets, fibrinogen, and plasminogen in patients with hepatic cirrhosis. J Lab Clin Med, 1982. 99(2): p. 217–30. [PubMed: 7061918]
11. Witters P, et al., Review article: blood platelet number and function in chronic liver disease and cirrhosis. Aliment Pharmacol Ther, 2008. 27(11): p. 1017–29. [PubMed: 18331464]
12. Laffi G, et al., Defective signal transduction in platelets from cirrhotics is associated with increased cyclic nucleotides. Gastroenterology, 1993. 105(1): p. 148–56. [PubMed: 8390377]

13. Laffi G, et al., Altered platelet function in cirrhosis of the liver: impairment of inositol lipid and arachidonic acid metabolism in response to agonists. Hepatology, 1988. 8(6): p. 1620–6. [PubMed: 3142812]
14. Laffi G, et al., Evidence for a storage pool defect in platelets from cirrhotic patients with defective aggregation. Gastroenterology, 1992. 103(2): p. 641–6. [PubMed: 1386051]
15. Ordinas A, et al., Existence of a platelet-adhesion defect in patients with cirrhosis independent of hematocrit: studies under flow conditions. Hepatology, 1996. 24(5): p. 1137–42. [PubMed: 8903388]
16. Owen JS, et al., Platelet lipid composition and platelet aggregation in human liver disease. J Lipid Res, 1981. 22(3): p. 423–30. [PubMed: 7240967]
17. Gowert NS, et al., Defective Platelet Activation and Bleeding Complications upon Cholestasis in Mice. Cell Physiol Biochem, 2017. 41(6): p. 2133–2149. [PubMed: 28441661]
18. Walter U, et al., Role of cyclic nucleotide-dependent protein kinases and their common substrate VASP in the regulation of human platelets. Adv Exp Med Biol, 1993. 344: p. 237–49. [PubMed: 8209791]
19. Michalopoulos GK, Grompe M, and Theise ND, Assessing the potential of induced liver regeneration. Nat Med, 2013. 19(9): p. 1096–7. [PubMed: 24013747]
20. Horstrup K, et al., Phosphorylation of focal adhesion vasodilator-stimulated phosphoprotein at Ser157 in intact human platelets correlates with fibrinogen receptor inhibition. Eur J Biochem, 1994. 225(1): p. 21–7. [PubMed: 7925440]
21. Nolte C, et al., Synergistic phosphorylation of the focal adhesion-associated vasodilator-stimulated phosphoprotein in intact human platelets in response to cGMP- and cAMP-elevating platelet inhibitors. Biochem Pharmacol, 1994. 48(8): p. 1569–75. [PubMed: 7980622]
22. Csanaky IL, et al., Role of hepatic transporters in prevention of bile acid toxicity after partial hepatectomy in mice. Am J Physiol Gastrointest Liver Physiol, 2009. 297(3): p. G419–33. [PubMed: 19497955]
23. Nomura S, et al., Cellular localization of thrombopoietin mRNA in the liver by in situ hybridization. Exp Hematol, 1997. 25(7): p. 565–72. [PubMed: 9216731]
24. Pereira J, et al., Platelet aging in vivo is associated with loss of membrane phospholipid asymmetry. Thromb Haemost, 1999. 82(4): p. 1318–21. [PubMed: 10544921]
25. Sorensen AL, et al., Role of sialic acid for platelet life span: exposure of beta-galactose results in the rapid clearance of platelets from the circulation by asialoglycoprotein receptor-expressing liver macrophages and hepatocytes. Blood, 2009. 114(8): p. 1645–54. [PubMed: 19520807]
26. Riswari SF and Tunjungputri RN, Desialylation of platelets induced by Von Willebrand Factor is a novel mechanism of platelet clearance in dengue. 2019. 15(3): p. e1007500.
27. Burmester H, et al., Thrombopoietin production in wild-type and interleukin-6 knockout mice with acute inflammation. J Interferon Cytokine Res, 2005. 25(7): p. 407–13. [PubMed: 16022585]
28. Kaser A, et al., Interleukin-6 stimulates thrombopoiesis through thrombopoietin: role in inflammatory thrombocytosis. Blood, 2001. 98(9): p. 2720–5. [PubMed: 11675343]
29. Peters M, et al., In vivo and in vitro activities of the gp130-stimulating designer cytokine Hyper-IL-6. J Immunol, 1998. 161(7): p. 3575–81. [PubMed: 9759879]
30. Mitchell O, et al., The pathophysiology of thrombocytopenia in chronic liver disease. Hepat Med, 2016. 8: p. 39–50. [PubMed: 27186144]
31. Sungaran R, Markovic B, and Chong BH, Localization and regulation of thrombopoietin mRNA expression in human kidney, liver, bone marrow, and spleen using in situ hybridization. Blood, 1997. 89(1): p. 101–7. [PubMed: 8978282]
32. Martin TG 3rd, et al., Thrombopoietin levels in patients with cirrhosis before and after orthotopic liver transplantation. Ann Intern Med, 1997. 127(4): p. 285–8. [PubMed: 9265428]
33. Koruk M, et al., Serum thrombopoietin levels in patients with chronic hepatitis and liver cirrhosis, and its relationship with circulating thrombocyte counts. Hepatogastroenterology, 2002. 49(48): p. 1645–8. [PubMed: 12397754]
34. Panasiuk A, et al., Reticulated platelets as a marker of megakaryopoiesis in liver cirrhosis; relation to thrombopoietin and hepatocyte growth factor serum concentration. Hepatogastroenterology, 2004. 51(58): p. 1124–8. [PubMed: 15239259]

35. Panasiuk A, et al., Inhibition of activated blood platelets by interferon alpha 2b in chronic hepatitis C. Hepatogastroenterology, 2004. 51(59): p. 1417–21. [PubMed: 15362767]
36. Peck-Radosavljevic M, et al., Thrombopoietin induces rapid resolution of thrombocytopenia after orthotopic liver transplantation through increased platelet production. Blood, 2000. 95(3): p. 795–801. [PubMed: 10648388]
37. Sezai S, et al., Regulation of hepatic thrombopoietin production by portal hemodynamics in liver cirrhosis. Am J Gastroenterol, 1998. 93(1): p. 80–2. [PubMed: 9448180]
38. Aref S, et al., Thrombopoietin (TPO) levels in hepatic patients with thrombocytopenia. Hematology, 2004. 9(5–6): p. 351–6. [PubMed: 15763973]
39. Lisman T, Leebeek FW, and de Groot PG, Haemostatic abnormalities in patients with liver disease. J Hepatol, 2002. 37(2): p. 280–7. [PubMed: 12127437]
40. Takahashi K, et al., Platelet and liver regeneration after liver surgery. Surg Today, 2019.
41. Intagliata NM, Davis JPE, and Caldwell SH, Coagulation Pathways, Hemostasis, and Thrombosis in Liver Failure. Semin Respir Crit Care Med, 2018. 39(5): p. 598–608. [PubMed: 30485890]
42. Elvers M, et al., Impaired alpha(IIb)beta(3) integrin activation and shear-dependent thrombus formation in mice lacking phospholipase D1. Sci Signal, 2010. 3(103): p. ra1. [PubMed: 20051593]
43. Deppermann C, et al., Macrophage galactose lectin is critical for Kupffer cells to clear aged platelets. J Exp Med, 2020. 217(4).
44. Blindenbacher A, et al., Interleukin 6 is important for survival after partial hepatectomy in mice. Hepatology, 2003. 38(3): p. 674–82. [PubMed: 12939594]
45. Cressman DE, et al., Liver failure and defective hepatocyte regeneration in interleukin-6-deficient mice. Science, 1996. 274(5291): p. 1379–83. [PubMed: 8910279]
46. Fazel Modares N, et al., IL-6 Trans-signaling Controls Liver Regeneration After Partial Hepatectomy. Hepatology, 2019. 70(6): p. 2075–2091. [PubMed: 31100194]
47. Fischer M, et al., I. A bioactive designer cytokine for human hematopoietic progenitor cell expansion. Nat Biotechnol, 1997. 15(2): p. 142–5. [PubMed: 9035138]
48. Behnke K, et al., B Cell-Mediated Maintenance of Cluster of Differentiation 169-Positive Cells Is Critical for Liver Regeneration. Hepatology, 2018. 68(6): p. 2348–2361. [PubMed: 29742809]

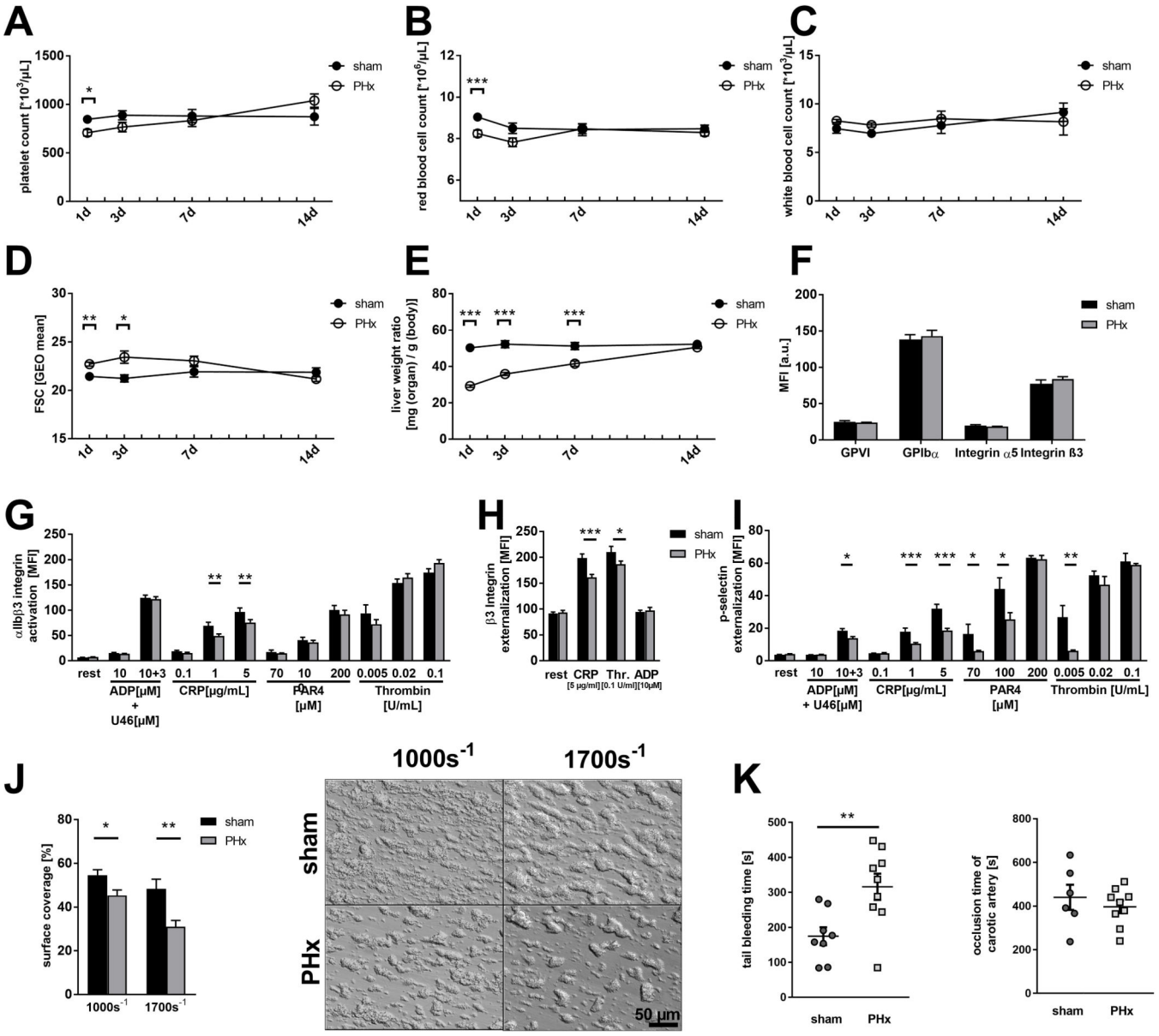

FIG 1.

Reduced total blood cell count and platelet activation defects in thrombosis and hemostasis 1 day after PHx. (A) Platelet count, (B) red blood cell count and (C) white blood cell count of C57Bl6/J mice undergoing partial hepatectomy. Sham operation served as control (n= 1d: 22 sham, 30 PHx, 3d: 22 sham, 26 PHx; 7d: 16 sham, 20 PHx; 14d: 8 sham, 12 PHx). (D) Platelet size of PHx and sham animals measured via flow cytometry using the geometric mean of GPIb positive platelets. (n= 1d: 10 sham, 14 PHx, 3d/7d/14d: 6 sham, 8 PHx). (E) Calculated liver weight ratio (n= 5 sham, 8 PHx). (F) Expression of indicated glycoproteins on the surface of platelets measured via mean fluorescence intensity (MFI) in flow cytometric analysis (n= 11 sham + 18 PHx). (G) Activation of αIIbβ3 integrin on the platelet surface with indicated agonists (n= 6 sham, 9 PHx). (H) Externalization of the β3 integrin subunit upon platelet stimulation (n= 6 sham, 8 PHx). (I) Externalization of P-

selectin on the platelet surface with indicated agonists (n= 6 sham, 9 PHx). (J) Thrombus formation on a collagen matrix under arterial shear rates with representative pictures (1000s $^{-1}$ n = 6 sham, 5 PHx; 1700s^{-1} n= 5 sham, 9 PHx). (K) *In vivo* analysis of hemostatic dysfunction via tail bleeding time (n= 8 sham, 9 PHx) and the Fe_3Cl induced injury of the carotid artery (n= 6 sham, 9 PHx). Depicted are mean values + s.e.m.; **P*<0.05, ***P*<0.01, ****P*<0.001 using *paired students t-test*.

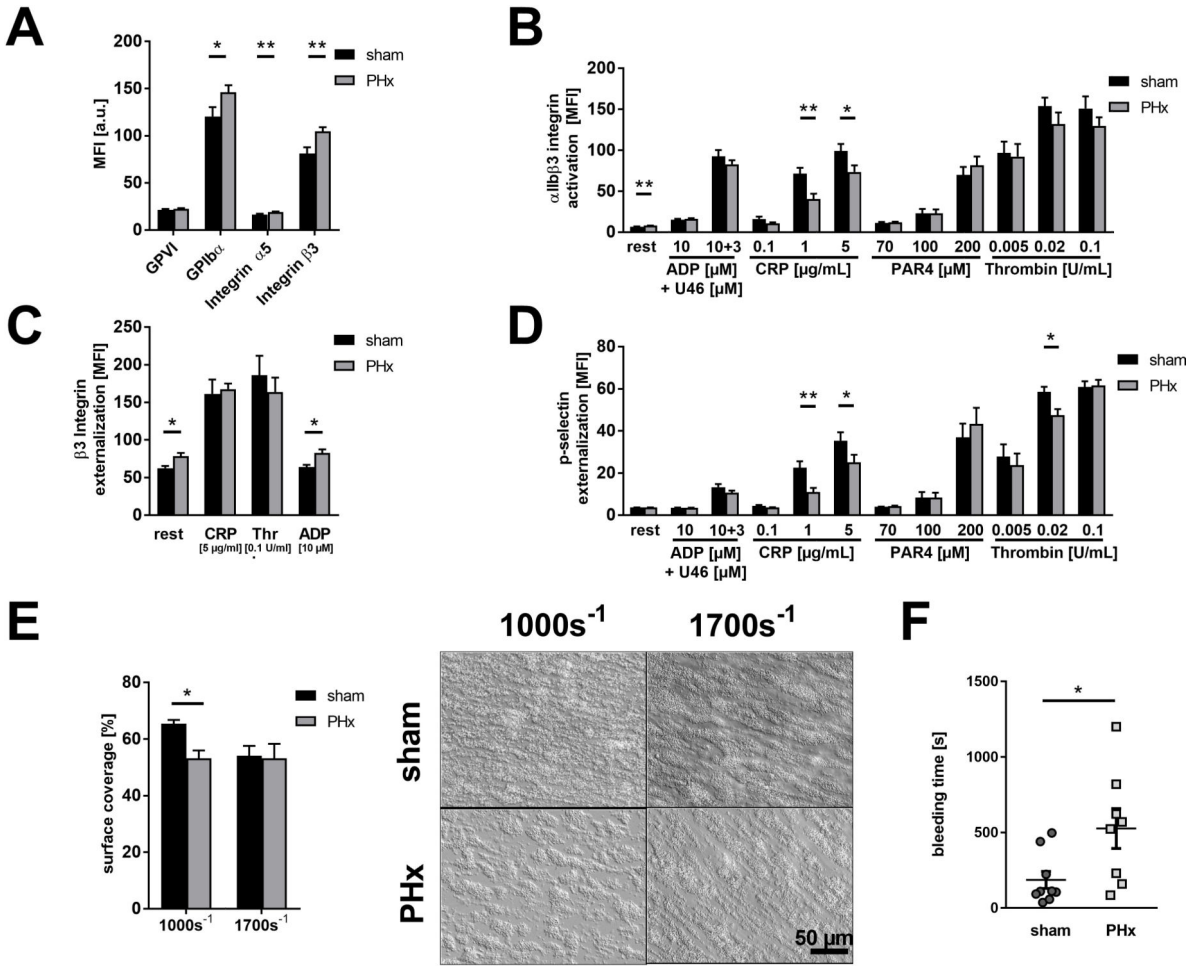

FIG. 2.

Platelet activation defects and reduced thrombus formation lead to bleeding complications 3 days after PHx. (A) Expression of indicated glycoproteins on the surface of platelets measured via MFI in flow cytometric analysis (n= 13 sham, 18 PHx). (B) Externalization of P-selectin on the platelet surface with indicated agonists (n= 9 sham, 12 PHx). (C) Externalization of the β3 Integrin subunit upon platelet stimulation (n= 8 sham, 9 PHx). (D) Activation of αIIbβ3 integrin on the platelet surface with indicated agonists (n= 9 sham, 12 PHx). (E) Thrombus formation on a collagen matrix under arterial shear rates with representative pictures ($1000s^{-1}$ and $1700s^{-1}$ n= 3 sham, 4 PHx). (F) *In vivo* analysis of hemostatic dysfunction via tail bleeding time (n= 9 sham, 8 PHx). Depicted are mean values + s.e.m.; **P*<0.05, ***P*<0.01 using *paired students t-test.*

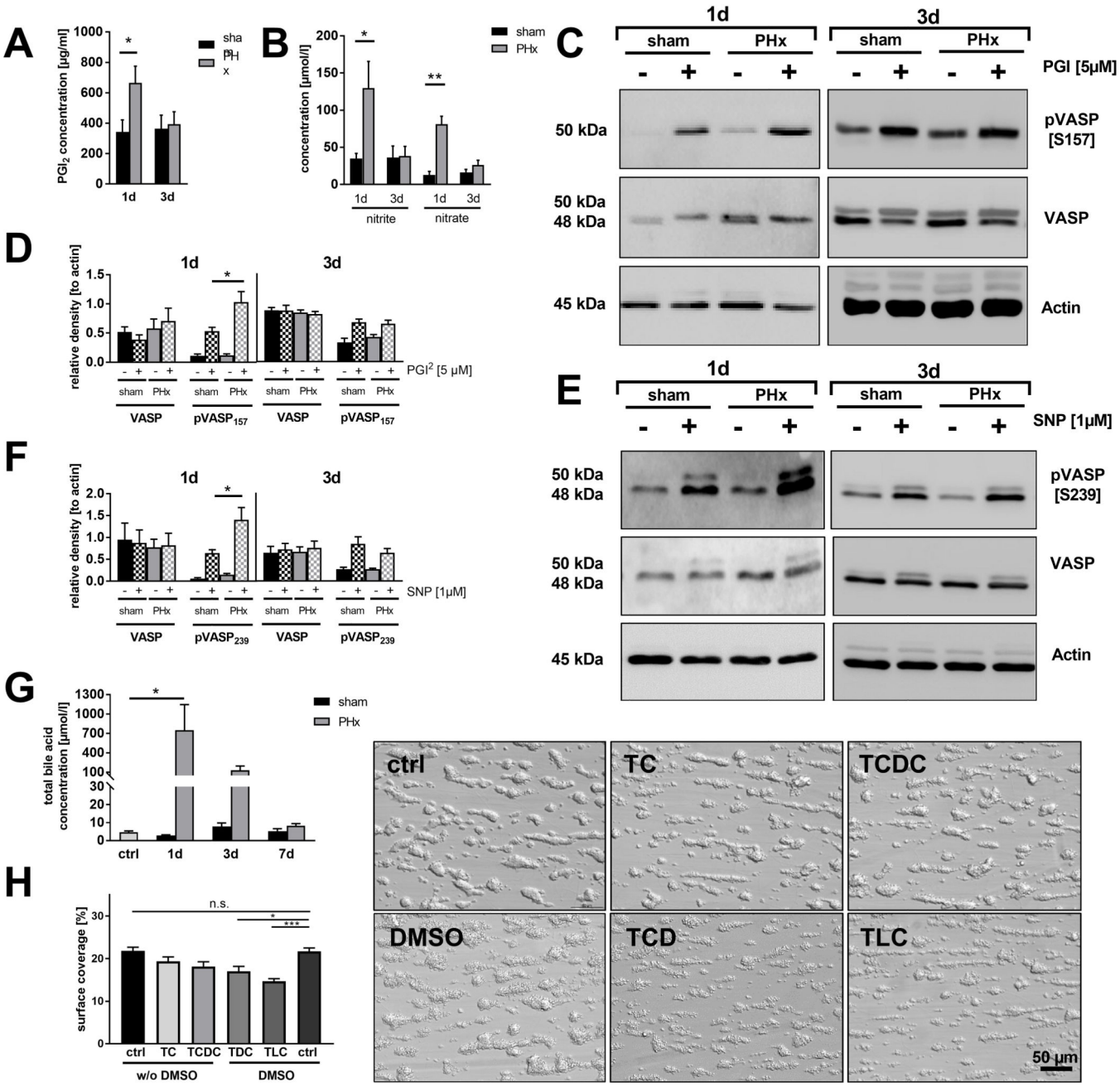

FIG. 3.

Platelet activation defects are provoked by enhanced plasma levels of nitric oxide, prostacyclin and bile acids. (A) PGI_2 plasma levels (n= 1d: 6 sham, 6 PHx; 3d: 3 sham, 4 PHx) and (B) indirect nitric oxide (NO) measurement via the plasma metabolites nitrite and nitrate 1 and 3 days after PHx (n= 1d: 4 sham, 4 PHx; 3d: 3 sham, 6 PHx). (C) Representative phosphorylation of vasodilator-stimulated phosphoprotein (VASP) at serine 157 in platelets stimulated with 5 µM PGI_2 (D) and densitometric analysis (n= 4 sham, 5 PHx). (E) Representative phosphorylation of vasodilator-stimulated phosphoprotein (VASP) at serine 239 and (F) densitometric analysis (n= 5 sham + 4 PHx). (G) Total bile acid content

in the serum of murine platelets (n = 5 control animals (ctrl); 1d: 3 sham, 6 PHx; 3d: 3 sham, 4 PHx; 7d: 3 sham, 3 PHx). (H) Thrombus formation under arterial shear rate ($1700s^{-1}$). Whole blood samples were pre-treated with different bile acids (conc. = 50 μM) for 30 min. Indicated bile acids are dissolved in 0.01 % DMSO. Representative images are shown for each treatment (n =6 per group). Depicted are mean values + s.e.m. $*P<0.05$, $**P<0.01$ using *paired students t-test.*

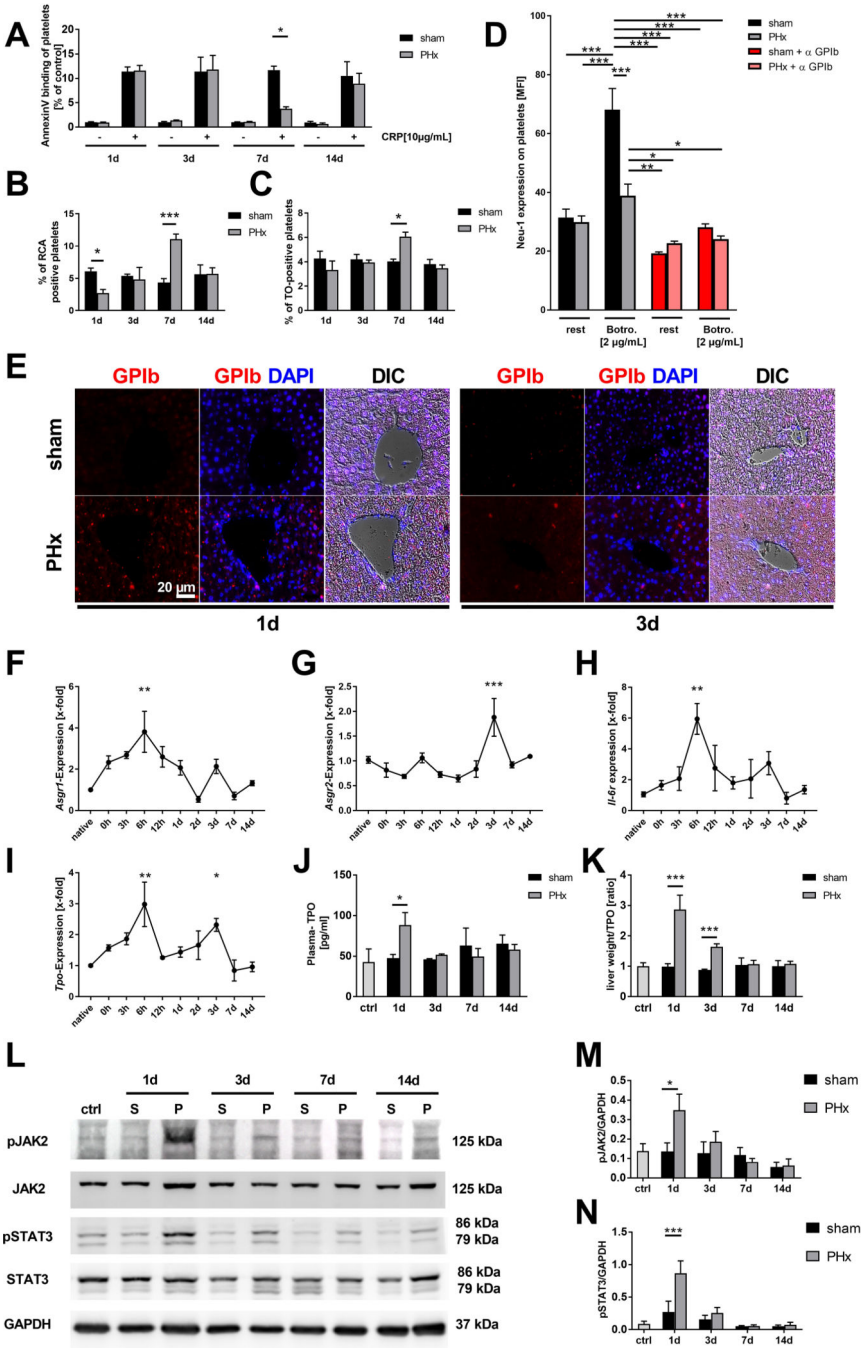

FIG. 4.

Efficiently restored TPO production is mediated via desialylated platelet uptake into the diseased liver by the AMR and JAK2 / STAT3 signaling. (A) AnnexinV-binding of GPIb positive platelets stimulated with CRP in regard to control group of each time point (n = 1+3d: 8 sham + 9 PHx; 7+14 d: 4 sham, 4 PHx). (B) Analysis of platelets positive for binding of the RCA-1 lectin (RCA-1 = *Ricinus communis* agglutinin-1) at indicated time points (n= 4 sham, 5 PHx). (C) Thiazol orange staining for RNA-rich, young GPIb positive platelets measured via flow cytometry (n= 8 sham + PHx for 1d + 3d; 4 sham, 5 PHx for

7+14d). (D) Neuraminidase (Neu)-1 expression at the platelet surface of sham and PHx operated mice was determined after Botrocetin (Botro.) and anti-GPIbα treatment of platelets (n = 6). (E) Representative images showing staining of paraffin embedded liver tissue sections for GPIb positive platelets at indicated time points. Nucleus staining performed with DAPI. Merge with differential interference contrast (DIC) is shown (n =4). (F-I) Gene expression of different target genes was analyzed using the $2^{-\Delta\Delta Ct}$ method (n= native animals 3; 0h: 4 animals; 3h-14d: 5–6 animals). (J) TPO level measured in plasma of mice with (K) calculated plasma TPO levels in regard to measured liver weight of the same animals (n = control 3; 1d = 6 sham, 7 PHx; 3/7/14d = 4 mice/group). (L) Representative immunoblots of total liver cell lysates using anti-pJAK2 and anti-JAK2 antibodies and anti-pSTAT3 and anti-STAT3 monoclonal antibodies. GAPDH was used as loading control. (M and N) Densitometric analysis of pJAK2 and pSTAT3 with regard to loading control (n=4). Depicted are mean values + s.e.m.; **P*<0.05, ***P*<0.01, ****P*<0.001 using ordinary *Two-Way ANOVA* with *Bonferroni's post-hoc test*, D was analysed using *Three-Way ANOVA with Bonferroni's post-hoc test*, F-I were analyzed using ordinary *One-Way ANOVA with Dunnett's post-hoc test.*

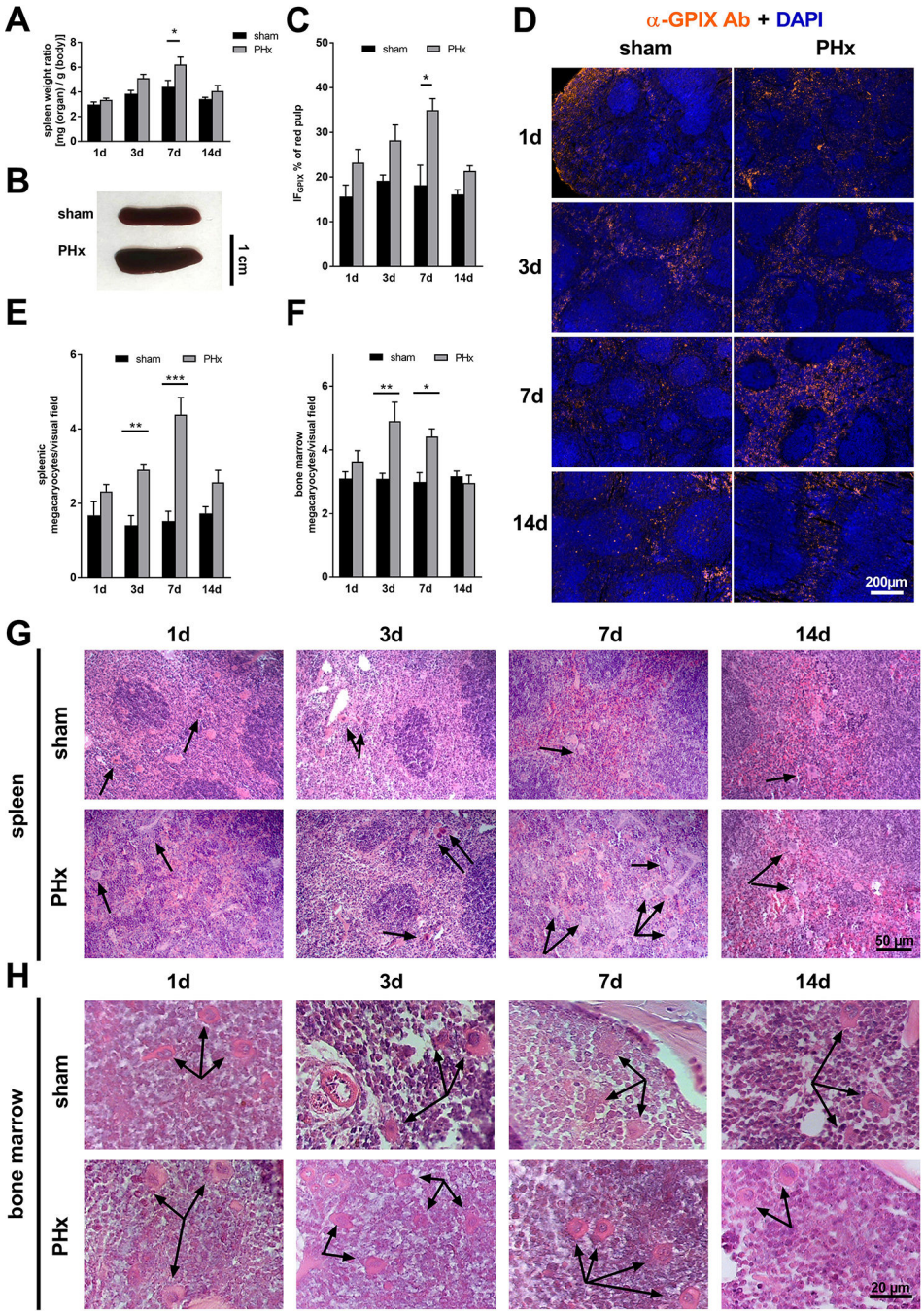

FIG. 5.

Elevated megakaryopoiesis is responsible for moderate splenomegaly after PHx. (A) Calculated spleen weight ratio (n = 1d: 10 sham, 14 PHx; 3d: 9 sham, 9 PHx; 7d: 8 sham, 10 PHx, 14d: 5 sham, 5 PHx) with (B) representative images of spleen tissue 7 days after operation. (C) Platelet sequestration in spleen sections of sham and PHx operated mice. A platelet specific marker (GPIX) was combined with DAPI staining to distinguish between red and withe pulp of the spleen. Total GPIX positive fluorescence area [IF_{GPIX}/ µm^2] of the red pulp of the spleen sections was determined with (D) representative IF staining of splenic

sequestration (n= 4). (E) Counted megakaryocytes in paraffin embedded spleen tissue (n = 5 sham, 5 PHx) and (F) bone marrow of the femur (n= 4 sham, 4 PHx). (G) Representative images from the spleen tissue and (H) the bone marrow tissue of the HE-staining. Arrowheads indicate megakaryocytes. Depicted are mean values + s.e.m.; *P<0.05, **P<0.01 using ordinary *Two-Way ANOVA with Bonferroni's post-hoc test.*

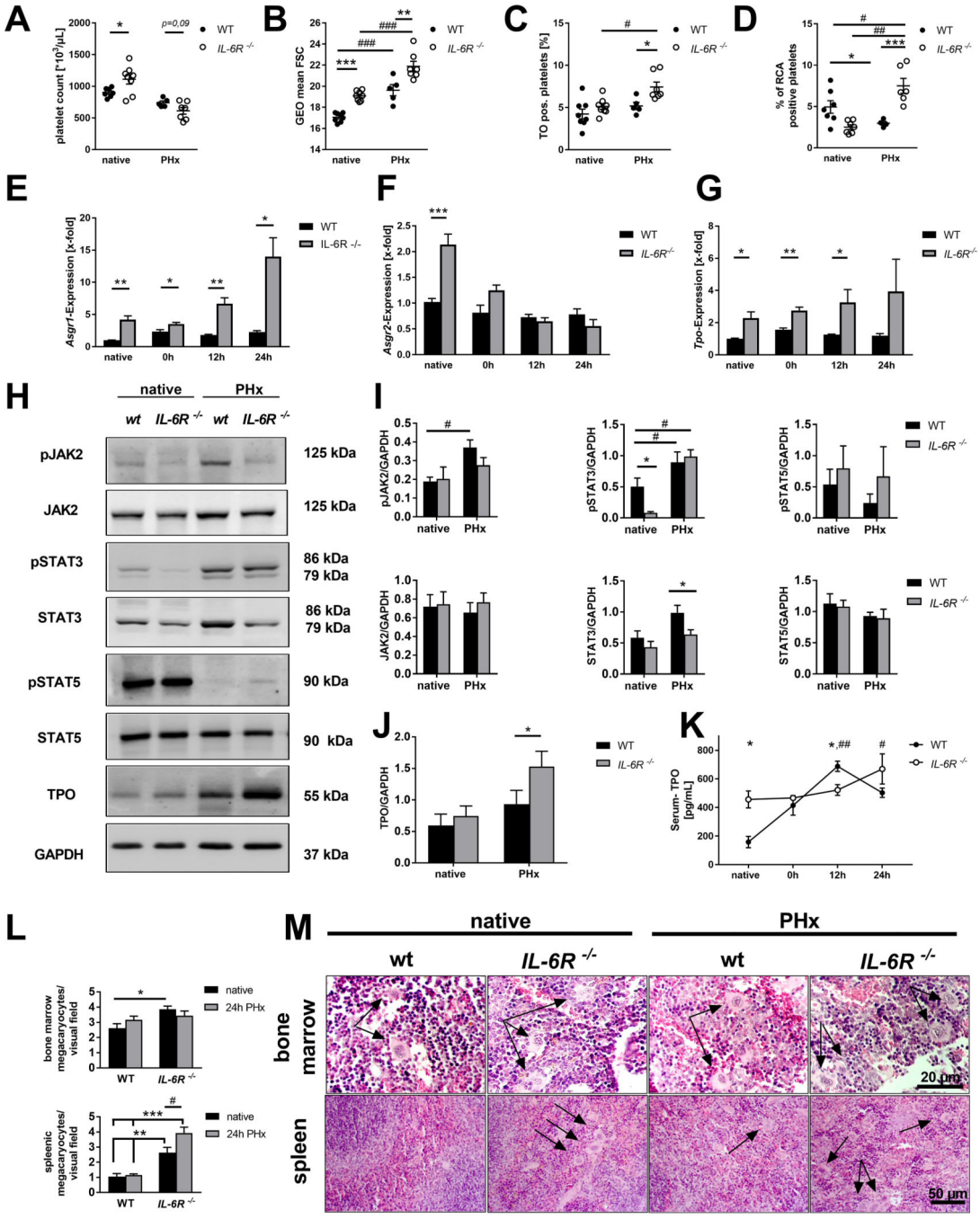

FIG. 6.

Elevated cytokine signaling controls TPO homeostasis in the remaining liver tissue via the IL-6R and STAT signaling *in vivo*. (A) Platelet count and (B) platelet size measured via geometric mean and (C) Thiazol orange staining of GPIb positive platelets of WT and *IL-6R* $^{-/-}$ mice before and 24h after PHx (n= native: 8 WT, 8 *IL-6R*$^{-/-}$; PHx: 5 WT, 7 *IL-6R*$^{-/-}$). (D) Analysis of platelets positive for binding of the RCA-1 lectin (n= native: 8 WT, 8 *IL-6R* $^{-/-}$; PHx: 5 WT, 7 *IL-6R*$^{-/-}$). (E-G) Gene expression was analysed using the $2^{-\Delta\Delta Ct}$ method (n= 4–5 WT/time point + 5 *IL-6R*$^{-/-}$/time point). (H) Representative immunoblots of total

liver cell lysates using anti-pJAK2 + anti-JAK2 antibodies, anti-pSTAT5 + STAT5 and anti-pSTAT3 + anti-STAT3 monoclonal antibodies. TPO polyclonal antibody was used with GAPDH as loading control (n= 5 for each group). (I) Densitometric analysis of the immunoblots for JAK2, STAT5 and STAT3 and their phospho-variant calculated with GAPDH as loading control. (J) Densitometric analysis of the immunoblots for TPO. (K) Serum concentration of TPO in WT and IL-6R −/− mice (n = 4 WT + 5 *IL-6R*$^{-/-}$). (L) Counted megakaryocytes in paraffin embedded bone marrow of femur tissue (n = 4 WT, 4 *IL-6R*$^{-/-}$) and spleen tissue (n= 5 WT, 5 *IL-6R*$^{-/-}$). (M) Representative images from bone marrow and spleen tissue of the HE-staining. Arrows indicate megakaryocytes. Depicted are mean values + s.e.m.; special characters indicate for difference between time points (#) or WT and *IL-6R*$^{-/-}$ *(*)*; #,* P<0.05, ##,** P<0.01, ###,*** P<0.001 using *paired students t-test*; *multiple t-test's* with the *Holm-Sidak method* (E-G) or *Two-Way ANOVA* with *Sidak's post-hoc* (K and L).